

LETTERS

A quantum gas microscope for detecting single atoms in a Hubbard-regime optical lattice

Waseem S. Bakr¹, Jonathon I. Gillen¹, Amy Peng¹, Simon Fölling¹ & Markus Greiner¹

Recent years have seen tremendous progress in creating complex atomic many-body quantum systems. One approach is to use macroscopic, effectively thermodynamic ensembles of ultracold atoms to create quantum gases and strongly correlated states of matter, and to analyse the bulk properties of the ensemble. For example, bosonic and fermionic atoms in a Hubbard-regime optical lattice^{1–5} can be used for quantum simulations of solid-state models⁶. The opposite approach is to build up microscopic quantum systems atom-by-atom, with complete control over all degrees of freedom^{7–9}. The atoms or ions act as qubits and allow the realization of quantum gates, with the goal of creating highly controllable quantum information systems. Until now, the macroscopic and microscopic strategies have been fairly disconnected. Here we present a quantum gas ‘microscope’ that bridges the two approaches, realizing a system in which atoms of a macroscopic ensemble are detected individually and a complete set of degrees of freedom for each of them is determined through preparation and measurement. By implementing a high-resolution optical imaging system, single atoms are detected with near-unity fidelity on individual sites of a Hubbard-regime optical lattice. The lattice itself is generated by projecting a holographic mask through the imaging system. It has an arbitrary geometry, chosen to support both strong tunnel coupling between lattice sites and strong on-site confinement. Our approach can be used to directly detect strongly correlated states of matter; in the context of condensed matter simulation, this corresponds to the detection of individual electrons in the simulated crystal. Also, the quantum gas microscope may enable addressing and read-out of large-scale quantum information systems based on ultracold atoms.

In Hubbard-regime optical lattice systems, an atomic quantum gas resides in the lowest Bloch band of a multi-dimensional array of lattice sites¹⁰. Strongly correlated quantum states, such as bosonic and fermionic Mott insulator states, have been created in such lattices^{2,4,5}, and the realization of quantum magnetism and *d*-wave superfluidity is being actively pursued^{6,11,12}. Experiments of this type have for the most part relied on measuring ensemble properties, such as global coherence and compressibility. Creating the possibility of probing the quantum gas with single atom/single lattice site resolution, in contrast, would allow experimenters to access the quantum gas on a single ‘qubit’ level and measure the particle–particle correlation functions that characterize strongly correlated quantum states.

The quantum gas microscope provides exactly this capability through an unprecedented combination of resolution and sensitivity. It is based on a number of innovations, such as solid immersion microscopy for cold atoms, a two-dimensional (2D) optical lattice in close vicinity to an optical surface, and the use of incoherent lattice light. The microscope enables the detection of single atoms with near-unity fidelity on single lattice sites of a short period optical lattice in the Hubbard model regime. Previously, site-resolved optical imaging of single atoms has been demonstrated in lattices with large

spacings (5 μm period)¹³ and in sparsely populated one-dimensional arrays¹⁴. Imaging of 2D arrays of ‘tubes’ with large occupations has been shown for smaller spacings with an electron microscope¹⁵ and optical imaging¹⁶ systems. For the described applications, however, a combination of high fidelity single atom detection and short lattice periods is important, which has not been previously achieved. The central feature of the Hubbard regime is that the tunnel coupling between sites and the on-site interaction must be comparable in strength, and should be larger than the temperature of the system. Small lattice spacings of the order of 500 nm are required to fulfil these requirements while also obtaining dynamical timescales much shorter than the lifetime of the Hubbard system. We demonstrate high fidelity site-resolved single atom detection in such a lattice.

The quantum gas microscope is based on a high aperture optical system, which simultaneously serves to generate lattice potentials and detect the atoms. By placing a 2D quantum gas only a few micrometres away from the front surface of this microscope, we are able to achieve a very high numerical aperture of NA = 0.8. As a result, we measure an optical resolution of ~ 600 nm (full-width at half-maximum, FWHM). Unlike typical optical lattice set-ups, we create the lattice potential by directly projecting a spatial light pattern^{16–20} onto the atom plane. A lithographically produced holographic mask and our high resolution optics allow us to generate arbitrary potential landscapes with sub-micrometre structures, opening the possibility of realizing a wide range of model Hamiltonians. Here we project a simple cubic lattice with a lattice constant of 640 nm, comparable to typical Hubbard-type lattice experiments. After loading the lattice, we can directly read out all (up to tens of thousands) lattice sites individually by imaging the light scattered by the atoms. The 2D geometry of the system enables imaging without line-of-sight integration, allowing for direct, reconstruction-free detection of densities²¹ in our system on a single atom level.

The central part of the set-up is the high resolution optical imaging system integrated with a 2D atom trap (Fig. 1). The imaging system consists of a long working distance microscope objective located outside the vacuum chamber which covers a numerical aperture of NA = 0.55. As an additional front lens of this imaging system, a hemispherical lens is placed inside the vacuum. With the quantum gas placed only a few micrometres from the superpolished flat bottom surface of the hemisphere, a ‘solid immersion’²² effect occurs, which increases the numerical aperture by the index of refraction of the hemisphere lens to NA = 0.8, yielding a diffraction limit of 500 nm at an imaging wavelength of 780 nm. The quantum gas of ⁸⁷Rb atoms is created in a hybrid surface trap based on evanescent and standing-wave light fields²³. Positioned between 1.5 and 3 μm from the surface, the quantum gas is deep in the 2D regime, with trap frequencies of 6 kHz in the vertical direction and 20 Hz in the horizontal plane.

The periodic potentials in the 2D plane are created by using the microscope optics to make a direct projection of a lithographically produced periodic mask that contains the lattice structure in the form

¹Harvard-MIT Center for Ultracold Atoms and Department of Physics, Harvard University, Cambridge, Massachusetts 02138, USA.

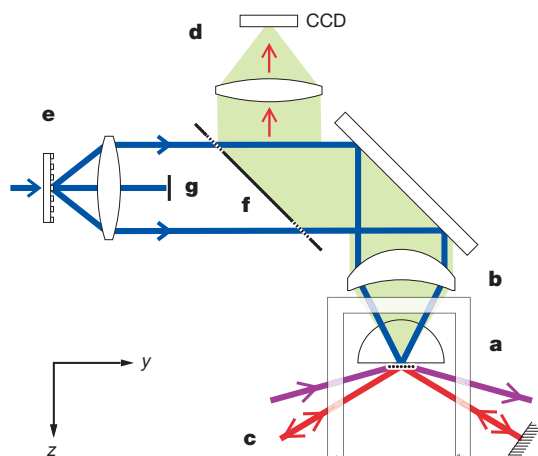


Figure 1 | Diagram of the quantum gas microscope. The two-dimensional atom sample (a) is located a few micrometres below the lower surface of a hemispherical lens inside the vacuum chamber. This lens serves to increase the numerical aperture (NA) of the objective lens outside the vacuum (b) by the index of refraction, from $NA = 0.55$ to $NA = 0.8$. The atoms are illuminated from the side by the molasses beams (c) and the scattered fluorescence light is collected by the objective lens and projected onto a CCD camera (d). A 2D optical lattice is generated by projecting a periodic mask (e) onto the atoms through the same objective lens via a beam splitter (f). The mask is a periodic phase hologram, and a beam stop (g) blocks the residual zeroth order, leaving only the first orders to form a sinusoidal potential.

of a phase hologram. This is in contrast to conventional optical lattice experiments in which lattice potentials are created by superimposing separate laser beams to create optical standing waves. The advantage of the new method is that the geometry of the lattice is directly given by the pattern on the mask. The imaged light pattern, and hence the potential landscape, can be arbitrary within the limits set by the available imaging aperture and by polarization effects that can arise due to the large aperture imaging beyond the paraxial limit. Here, we create blue detuned square lattice potentials with a periodicity $a = 640$ nm and an overall Gaussian envelope. A major additional advantage is the fact that the lattice geometry is not dependent on the wavelength²⁰, apart from diffraction limits and chromatic aberrations in the lens for large wavelength changes. This allows us to use spectrally wide ‘white’ light with a short coherence length to reduce unwanted disorder from stray light interference. With a light source centred around 758 nm, we generate a conservative lattice potential with a lattice depth of up to $35 E_{\text{rec}}$ where $E_{\text{rec}} = \hbar^2/8ma^2$ is the recoil energy of the effective lattice wavelength, with m the mass of ^{87}Rb .

The projection method also enables us to dynamically change the wavelength of the lattice light without changing the lattice geometry. This is important, as we strongly increase the lattice depth for site-resolved imaging in order to suppress diffusion of the atoms between sites due to recoil heating by the imaging light¹³. For this, we switch the light in the 2D lattice and the vertical standing wave to near-resonant narrow band light, increasing the lattice depth to $5,500 E_{\text{rec}}$ (to $380 \mu\text{K}$). The main use of the microscope set-up is the collection of fluorescence light and high-resolution imaging of the atoms. With the atoms pinned to the deep lattice, we illuminate the sample with red detuned near-resonant light in an optical molasses configuration, which simultaneously provides sub-Doppler cooling^{24,25}. Figure 2 shows a typical image obtained by loading the lattice with a very dilute cloud, showing the response of individual atoms. The spot function of a single atom can be directly obtained from such images. We measure a typical single atom emission FWHM size as 570 nm and 630 nm along the x and y direction, respectively, which is close to the theoretical minimum value of ~ 520 nm (Fig. 3). This minimum is given by the diffraction limit from the objective combined with the finite size of the camera

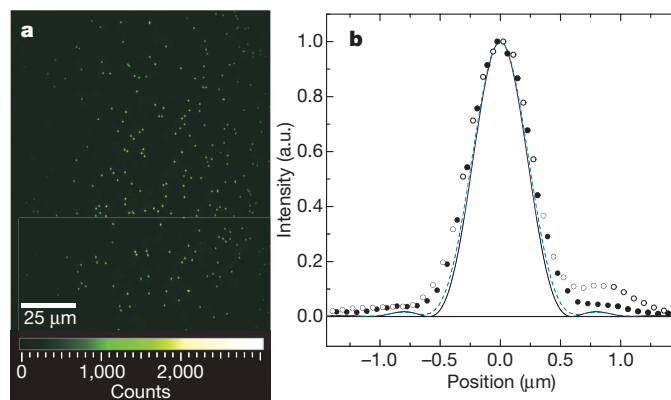


Figure 2 | Imaging single atoms. a, Field of view with sparse site occupation. b, Response of a single atom, derived from sparse images: shown are horizontal (filled circles) and vertical (open circles) profiles through the centre of the image generated by a single atom. The black line shows the expected Airy function for a perfect imaging system with a numerical aperture of 0.8. The blue dashed line denotes the profile expected from a single atom, taking into account only the finite width of the CCD pixels and the finite extension of the probability distribution of the atom’s location. The data are from the responses of 20 atoms in different locations within the field of view which have been precisely superimposed by subpixel shifting before averaging.

pixels and the expected extent of the atom’s on-site probability distribution within the lattice site during the imaging process. As the same high-resolution optics are used to generate both the lattice and the image of the atoms on the CCD camera, the imaging system is very stable with respect to the lattice, which is important for single-site addressing²⁶. The observed drifts in the 2D plane are very low, less than 10% of the lattice spacing in one hour with shot to shot fluctuations of less than 15% r.m.s.

Pair densities within multiply occupied lattice sites are very high due to the strong confinement in the lattice. When resonantly illuminated, such pairs undergo light assisted collisions and leave the trap within a time of the order of $100 \mu\text{s}$, long before they emit sufficient photons to be detected²⁷. Therefore the remaining number

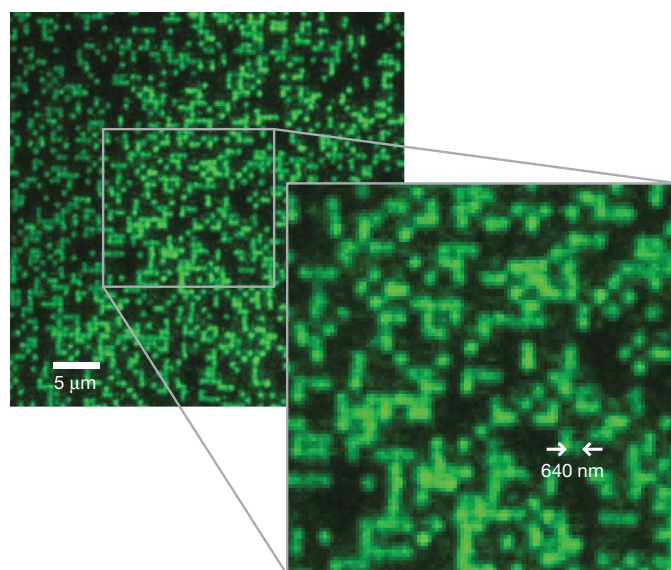


Figure 3 | Site-resolved imaging of single atoms on a 640-nm-period optical lattice, loaded with a high density Bose–Einstein condensate. Inset, magnified view of the central section of the picture. The lattice structure and the discrete atoms are clearly visible. Owing to light-assisted collisions and molecule formation on multiply occupied sites during imaging, only empty and singly occupied sites can be seen in the image.

of atoms per site is equal to the parity of the original atom number before illumination, as long as the initial occupation is small. For our molasses parameters, the collected number of photons can be up to 2×10^4 per atom per second, and the exposure times are typically between 200 and 1,000 ms, limited by the loss of single atoms from the trap which reduces the detection fidelity. The $1/e$ lifetime is ~ 30 s, which is consistent with loss due to collisions with hot atoms in the background gas.

Figure 3 shows an image obtained by loading a dense Bose–Einstein condensate. The fast ramp-up of the pinning lattice within 1.5 ms switches off tunnelling and projects the superfluid state wavefunction onto Poisson distributed on-site occupations with more than one atom per lattice site in the centre of the trap. Owing to the removal of pairs the occupation detected is lowered, typically to 42%. The images are analysed by identifying the lattice geometry and fitting point spread functions (obtained separately by analysing images from sparsely filled lattices) to each lattice point. As the background signal is weak and smooth due to the 2D geometry, we thus obtain the total number of scattered photons per lattice site as a simple way of determining the presence of an atom. Figure 4 shows the histogram of photon counts for the central region of several images with an average filling of 34%. For these pictures with long exposure times, the fidelity of identifying atoms at a given lattice site is 98%, limited by the losses occurring during the integration time. To verify that the atom distribution is preserved during imaging, we have recorded sequences of consecutive images spanning a total detection period of several seconds, during which no significant hopping occurs.

In conclusion, we have demonstrated site resolved high fidelity imaging of thousands of individual atoms in a Hubbard-regime optical lattice. A complete set of degrees of freedom of each of them is determined through preparation and measurement. Such detection opens many new possibilities. Strongly correlated quantum states, such as the Mott insulator and antiferromagnetic states, could be directly detected, making it possible to determine results of quantum simulations on a single ‘qubit’ level. In our lattice configuration, the Mott transition is expected at a lattice depth of $\sim 12 E_{\text{rec}}$ with a tunnel coupling strength J of 20 Hz at the transition point, similar to the parameters in ref. 21. Single atom detection would then enable the precise measurement of entropy or temperature via the direct detection of defects. Similarly, such imaging is an enabling method for quantum information applications. Based on a Mott insulator state and time-varying state-dependent potentials, maximally entangled cluster states of tens of atoms have been created²⁸, which could be used as a resource for quantum computations²⁹. For detecting or exploiting this entanglement, however, single-site readout and manipulation are essential. Generating our lattice potentials by direct projection of a 2D

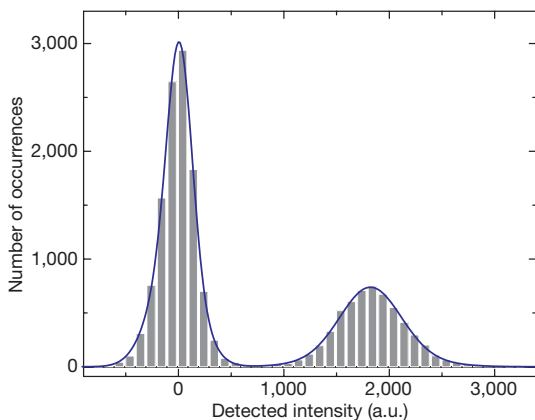


Figure 4 | Histogram showing the brightness distribution of lattice sites for an exposure time of 1 s. The left peak corresponds to empty sites (background subtracted), the right peak to those occupied by a single atom. The blue line denotes a fit to the data using a double Gaussian function for each of the two peaks. a.u., arbitrary units.

mask gives us the additional advantage of full control over the lattice geometry on a single-site level. The method can be generalized to create arbitrary potential landscapes, including spin-dependent ones, for realizing a large class of model Hamiltonians. Local manipulation could also enable new cooling schemes³⁰ for reaching temperatures low enough to study quantum magnetism and d -wave superfluidity.

METHODS SUMMARY

A 2D Bose–Einstein condensate of ^{87}Rb is created by loading a three-dimensional (3D) cloud into a hybrid surface trap, described in detail in ref. 23. The 2D trap is formed by using a magnetic gradient to push a spherical condensate against a repulsive dipole potential due to an evanescent wave from a blue-detuned beam totally internally reflected inside the hemispherical lens. The resulting pancake-shaped condensate is then loaded into a single well of a one-dimensional (1D) far off-resonant lattice with nodal planes parallel to the glass spaced at 1.5 μm . The final geometry has axial and transverse confinements of 6 kHz and 20 Hz, respectively.

A square lattice light pattern created using holographic masks is projected onto the atom plane through the high resolution objective. The lattice spacing in the atom plane is 640 nm. By an appropriate choice of polarizations and frequencies, the lattice light is linearly polarized everywhere. This is essential to avoid effective magnetic fields in the case of near resonant light that can interfere with polarization gradient cooling in the imaging molasses. We create a conservative lattice by illuminating the holograms with blue detuned broadband light at 22 nm from the D2 transition. For imaging, we switch on a superposed pinning lattice with a depth of 380 μK , generated using the same holograms with a separate narrow band light source detuned 32 GHz from the D1 line. The atoms are then illuminated in a molasses configuration at 80 MHz from the D2 line and imaged by collecting the scattered photons onto a CCD. The photon collection efficiency is $\sim 10\%$.

Full Methods and any associated references are available in the online version of the paper at www.nature.com/nature.

Received 20 July; accepted 3 September 2009.

- Jaksch, D., Bruder, C., Cirac, J. I., Gardiner, C. W. & Zoller, P. Cold bosonic atoms in optical lattices. *Phys. Rev. Lett.* **81**, 3108–3111 (1998).
- Greiner, M., Mandel, O., Esslinger, T., Hansch, T. & Bloch, I. Quantum phase transition from a superfluid to a Mott insulator in a gas of ultracold atoms. *Nature* **415**, 39–44 (2002).
- Kohl, M., Moritz, H., Stoferle, T., Gunter, K. & Esslinger, T. Fermionic atoms in a three dimensional optical lattice: observing Fermi surfaces, dynamics, and interactions. *Phys. Rev. Lett.* **94**, 080403 (2005).
- Jordens, R., Strohmaier, N., Gunter, K., Moritz, H. & Esslinger, T. A Mott insulator of fermionic atoms in an optical lattice. *Nature* **455**, 204–207 (2008).
- Schneider, U. *et al.* Metallic and insulating phases of repulsively interacting fermions in a 3D optical lattice. *Science* **322**, 1520–1525 (2008).
- Bloch, I., Dalibard, J. & Zwirger, W. Many-body physics with ultracold gases. *Rev. Mod. Phys.* **80**, 885–964 (2008).
- Schrader, D. *et al.* Neutral atom quantum register. *Phys. Rev. Lett.* **93**, 150501 (2004).
- Blatt, R. & Wineland, D. J. Entangled states of trapped atomic ions. *Nature* **453**, 1008–1014 (2008).
- Urban, E. *et al.* Observation of Rydberg blockade between two atoms. *Nature Phys.* **5**, 110–114 (2009).
- Jaksch, D. & Zwirger, W. The cold atom Hubbard toolbox. *Ann. Phys.* **315**, 52–79 (2005).
- Duan, L.-M., Demler, E. & Lukin, M. D. Controlling spin exchange interactions of ultracold atoms in optical lattices. *Phys. Rev. Lett.* **91**, 090402 (2003).
- Trotzky, S. *et al.* Time-resolved observation and control of superexchange interactions with ultracold atoms in optical lattices. *Science* **319**, 295–299 (2008).
- Nelson, K., Li, X. & Weiss, D. Imaging single atoms in a three-dimensional array. *Nature Phys.* **3**, 556–560 (2007).
- Karski, M. *et al.* Nearest-neighbor detection of atoms in a 1D optical lattice by fluorescence imaging. *Phys. Rev. Lett.* **102**, 053001 (2009).
- Gericke, T., Wurtz, P., Reitz, D., Langen, T. & Ott, H. High-resolution scanning electron microscopy of an ultracold quantum gas. *Nature Phys.* **4**, 949–953 (2008).
- Itah, A. *et al.* Direct observation of number squeezing in an optical lattice. Preprint at (<http://arxiv.org/abs/0903.3282>) (2009).
- Grier, D. G. A revolution in optical manipulation. *Nature* **424**, 810–816 (2003).
- Newell, R., Sebby, J. & Walker, T. G. Dense atom clouds in a holographic atom trap. *Opt. Lett.* **28**, 1266–1268 (2003).
- Bergamini, S. *et al.* Holographic generation of microtrap arrays for single atoms by use of a programmable phase modulator. *J. Opt. Soc. Am. B* **21**, 1889–1894 (2004).

20. Brickman Soderberg, K., Gemelke, N. & Chin, C. Ultracold molecules: vehicles to scalable quantum information processing. *N. J. Phys.* **11**, 055022 (2009).
21. Gemelke, N., Zhang, X., Hung, C. & Chin, C. *In situ* observation of incompressible Mott-insulating domains in ultracold atomic gases. *Nature* **460**, 995–998 (2009).
22. Mansfield, S. M. & Kino, G. S. Solid immersion microscope. *Appl. Phys. Lett.* **57**, 2615–2616 (1990).
23. Gillen, J. I., Bakr, W. S., Peng, A., Unterwadtzer, P., Fölling, S. & Greiner, M. Two-dimensional quantum gas in a hybrid surface trap. *Phys. Rev. A* **80**, 021602(R) (2009).
24. Wineland, D. J., Dalibard, J. & Cohen-Tannoudji, C. Sisyphus cooling of a bound atom. *J. Opt. Soc. Am. B* **9**, 32–42 (1992).
25. Winoto, S. L., DePue, M., Bramall, N. E. & Weiss, D. S. Laser cooling at high density in deep far-detuned optical lattices. *Phys. Rev. A* **59**, R19–R22 (1999).
26. Würtz, P., Langen, T., Gericke, T., Koglbauer, A. & Ott, H. Experimental demonstration of single-site addressability in a two-dimensional optical lattice. *Phys. Rev. Lett.* **103**, 080404 (2009).
27. DePue, M. T., McCormick, C., Winoto, S. L., Oliver, S. & Weiss, D. S. Unity occupation of sites in a 3D optical lattice. *Phys. Rev. Lett.* **82**, 2262–2265 (1999).
28. Mandel, O. *et al.* Controlled collisions for multi-particle entanglement of optically trapped atoms. *Nature* **425**, 937–940 (2003).
29. Raussendorf, R. & Briegel, H. J. A one-way quantum computer. *Phys. Rev. Lett.* **86**, 5188–5191 (2001).
30. Bernier, J. *et al.* Cooling fermionic atoms in optical lattices by shaping the confinement. *Phys. Rev. A* **79**, 061601 (2009).

Acknowledgements We are grateful for discussions with D. Weiss and V. Vuletic and thank P. Unterwadtzer, E. Su and J. Brachmann for experimental assistance during the early stage of the experiment. We thank D. Weiss for sharing the lens design of the objective lens. This work was funded by grants from the NSF, AFOSR MURI, DARPA, an Alfred P. Sloan Fellowship to M.G., and an NSF Fellowship to J.I.G.

Author Contributions All authors contributed to the design and building of the set-up and taking of the data. W.S.B. and S.F. analysed the data and W.S.B., S.F. and M.G. wrote the manuscript.

Author Information Reprints and permissions information is available at www.nature.com/reprints. Correspondence and requests for materials should be addressed to M.G. (greiner@physics.harvard.edu).

METHODS

Hybrid surface trap. The hybrid surface trap, described in detail elsewhere²³, is loaded in a two-step sequence. First, a Bose–Einstein condensate created in a spherical magnetic trap is moved against the flat, superpolished glass surface. Close to the glass, it experiences a repulsive dipole potential due to an evanescent wave from a 767 nm blue detuned beam with a spectral width of 2 nm which is totally internally reflected inside the glass. This results in tight axial confinement with trap frequencies of typically 900 Hz. The weak axial confinement of 20 Hz is provided by the magnetic trap. In order to increase the axial confinement to the final value, the 2D gas is transferred into a vertical standing wave generated by a blue-detuned far off-resonant beam reflected at 15° from the trapping surface. Using radio-frequency forced evaporative cooling, we achieve nearly pure condensates in the 2D trap, as verified by time-of-flight imaging and matter wave interference²³.

Optical lattice projection. We create arbitrary potential landscapes by imaging holographic masks onto the atom plane. In this experiment, we use two binary phase holograms to create sinusoidal potentials along the x and y axes respectively. The holograms are illuminated with linearly polarized light, polarized perpendicular to the plane of diffraction. The two light paths are combined with a polarizing beam splitter cube. The far off-resonant lattice is created with light from a femto-second laser, with a spectral width of 3 nm centred at 758 nm. The short coherence length improves the quality of the transverse lattice potential owing to the elimination of uncontrolled interference with stray light²³. The lattice potential produced by the holograms is given by $V(x,y) = V_0(\sin^2(kx) + \sin^2(ky))$, where the periodicity of the lattice is given by $a = \pi/k = 640$ nm and V_0 , the depth of the potential, can reach up to $35 E_{\text{rec}}$. For imaging, we increase the lattice depth to 5,500

E_{rec} (0.38 mK) by illuminating the lattice holograms with light from a continuous wave Ti:sapphire laser detuned 32 GHz to the blue of the D1 transition of ^{87}Rb , without changing the lattice geometry. This pinning lattice is linearly polarized everywhere to avoid effective magnetic fields that interfere with the polarization gradient cooling during imaging. This is achieved using the proper choice of polarizations and by introducing frequency differences of at least 80 MHz between lattice axes to time average the interference between them. Near resonant light from the same source is used to simultaneously increase the lattice depth in the axial direction to 3 mK.

Fluorescence imaging. After the atoms are pinned, we image the atoms by illuminating them with light detuned 80 MHz to the red of the $F = 2$ to $F' = 3$ transition of the D2 line, where F and F' denote the hyperfine manifold in the ground and excited state, respectively. The light is in an optical molasses configuration which simultaneously provides illumination and cooling. One beam enters from the y axis and is reflected off the trapping surface at an angle of 15° and then retroreflected with perpendicular polarization along the same path. This results in polarization and intensity gradients along the y direction and the vertical. An additional beam enters along the x axis which generates polarization gradient components along this axis by interference with the retroreflected beam. In addition, to avoid cooling inefficiencies due to low polarization gradients on some lattice sites, we frequency offset the molasses beams by 7 kHz for temporal averaging of the cooling pattern.

The photons scattered by the optical molasses are collected for fluorescence detection of the atoms. The solid angle of the imaging system leads to a collection efficiency of 20%, such that we expect a total photon collection efficiency of ~10% including the quantum efficiency of the CCD camera (Andor Ixon DU888). The effective pixel size in the object plane is 167 nm.